Title

Contribution of Pulmonary CYP-mediated Bioactivation of Naphthalene to Airway Epithelial Injury in the Lung

Journal

Toxicological Sciences, 177(2)

ISSN

1096-6080

Authors

Kovalchuk, Nataliia
Zhang, Qing-Yu
Van Winkle, Laura
et al.

Publication Date

2020-10-01

DOI

10.1093/toxsci/kfaa114

Peer reviewed

OXFORD

SOT | Society of Toxicology
academic.oup.com/toxsci

TOXICOLOGICAL SCIENCES, 177(2), 2020, 334–346

doi: 10.1093/toxsci/kfaa114
Advance Access Publication Date: 16 July 2020
Research Article

Contribution of Pulmonary CYP-mediated Bioactivation of Naphthalene to Airway Epithelial Injury in the Lung

Nataliia Kovalchuk,*,† Qing-Yu Zhang,*,† Laura Van Winkle ,‡,1 and Xinxin Ding*,1

*Department of Pharmacology and Toxicology, College of Pharmacy, University of Arizona, Tucson, Arizona 85721; †Wadsworth Center, New York State Department of Health, and School of Public Health, State University of New York at Albany, Albany, New York 12201; and ‡Center for Health and the Environment and Department of Anatomy, Physiology and Cell Biology, School of Veterinary Medicine, UC Davis, Davis, California 95616

[1]To whom correspondence should be addressed at Dr. Laura Van Winkle, Center for Health and the Environment, University of California at Davis, Davis, CA 95616. E-mail: lsvanwinkle@ucdavis.edu and Dr. Xinxin Ding, Department of Pharmacology and Toxicology, College of Pharmacy, University of Arizona, Tucson, AZ 85721, E-mail: xding@pharmacy.arizona.edu.

ABSTRACT

Previous studies have established that cytochrome P450 enzymes (CYPs) in both liver and lung are capable of bioactivating naphthalene (NA), an omnipresent air pollutant and possible human carcinogen, *in vitro* and *in vivo*. The aim of this study was to examine the specific contribution of pulmonary CYPs in airway epithelial cells to NA-induced airway toxicity. We used a lung-*Cpr*-null mouse model, which undergoes doxycycline-induced, Cre-mediated deletion of the *Cpr* (a redox partner of all microsomal CYPs) gene specifically in airway epithelial cells. In 2-month-old lung-*Cpr*-null mice, *Cpr* deletion occurred in 75%–82% of epithelial cells of conducting airways. The extent of NA-induced acute lung toxicity (as indicated by total protein concentration and lactate dehydrogenase activity in bronchoalveolar lavage fluid collected at 24-h after initiation of a 4-h, nose-only, 10-ppm NA inhalation exposure) was substantially lower (by 37%–39%) in lung-*Cpr*-null mice, compared with control littermates. Moreover, the extent of cellular proliferation (as indicated by 5-bromo-2′-deoxyuridine incorporation) was noticeably lower in both proximal and distal airways (by 59% and 65%, respectively) of NA-treated lung-*Cpr*-null mice, compared with control littermates, at 2-day post-NA inhalation exposure. A similar genotype-related difference in the extent of postexposure cell proliferation was also observed in mice exposed to NA via intraperitoneal injection at 200 mg/kg. These results directly validate the hypothesis that microsomal CYP enzymes in airway epithelial cells play a large role in causing injury to airway epithelia following exposure to NA via either inhalation or intraperitoneal route.

Key words: naphthalene; cytochrome P450; P450 reductase; inhalation exposure; airway toxicity.

Naphthalene (NA) is a ubiquitous and highly abundant environmental pollutant (Kakareka and Kukharchyk, 2003; USEPA, 1986; Witschi *et al.*, 1997) and a Possible Human Carcinogen (group 2B) (IARC, 2002). NA has been the subject of intense study, due to prevalent exposure in the general population and the current uncertainty in risk assessment, and because it is a representative of many extensively metabolized small aromatic hydrocarbons, to which humans are widely exposed. Furthermore, much of NA's biotransformation pathway is understood in the lung, which makes NA a good model compound to probe mechanisms of xenobiotic toxicity, including the interplay between target organ and systemic metabolism and between metabolic

activation and detoxification (Buchholz *et al.*, 2019; Carratt *et al.*, 2019a,b; Ding *et al.*, 2018; Kovalchuk *et al.*, 2017, 2019; Li *et al.*, 2017).

Although the airway epithelium consists of many different cell types, the xenobiotic-metabolizing enzymes are predominantly localized in nonciliated (Club) cells in conducting airways and type II cells in the alveolus. Whereas chronic (2-year) exposure to NA induces nasal tumors in rats at 10 ppm and lung tumors in mice at 30 ppm (Abdo *et al.*, 1992, 2001), acute exposure to either inhaled or circulating NA preferentially injures Club cells (Plopper *et al.*, 1992a,b; West *et al.*, 2001). Isolated Club cells and lung explants from microdissected airways are fully capable of bioactivating NA and undergo NA-induced cytotoxicity (Boland *et al.*, 2004; Buckpitt *et al.*, 1995; Chichester *et al.*, 1994; Van Winkle *et al.*, 1996). The perfusion of isolated mouse lung with either NA (5 μmol over 60 min) or naphthalene-oxide (0.12 μmol over 60 min) resulted in morphological changes of bronchiolar epithelium, mostly in nonciliated Club cells. These *in vitro* and *ex vivo* studies provided strong evidence that Club cells play important roles in NA-induced airway cytotoxicity.

NA is metabolized by cytochrome P450 (CYPs) to the highly reactive NA oxide, which can be further metabolized to several other reactive metabolites, including NA 1,2- and 1,4-quinones (Carratt *et al.*, 2016). These reactive metabolites are formed in the liver, as well as in the lung. Thus, an important question regarding mechanisms of toxicity is whether metabolites generated in the liver can cause toxicity in the lung. Studies using *Cyp*-null mice indicated that both CYP2A and CYP2F play a role in NA bioactivation and airway toxicity (Hu *et al.*, 2014; Li *et al.*, 2011, 2017). However, these P450 enzymes are present in both the liver and the lung in mice. Studies using a liver-*Cpr*-null (LCN) mouse (Kovalchuk *et al.*, 2017) provided evidence for a role of liver generated NA metabolites in NA-induced lung toxicity. However, the relative contributions of CYP enzymes in the liver and lung to NA's lung toxicity are not clear, in part because the prior *in vivo* studies using the LCN mice were complicated by simultaneous effects of hepatic *Cpr* ablation on systemic NA clearance and hepatic NA bioactivation (Kovalchuk *et al.*, 2017, 2019).

A complementary approach to using a LCN mice is to employ a mouse model with selective ablation of P450 activity in the lung, which would allow us to demonstrate the specific contributions of airway epithelial cell P450 enzymes to NA lung toxicity *in vivo*, presumably with little to no effect on systemic disposition of NA, which is dominated by liver metabolism. Here, we have utilized a lung-*Cpr*-null mouse model (Weng *et al.*, 2007) to test the hypothesis that microsomal CYP enzymes in airway epithelial cells play an important role in the bioactivation and airway epithelial injury induced by NA. Initial studies were conducted in mice exposed to NA via intraperitoneal injection, a commonly employed route for most mechanistic studies on NA toxicity in the lung, at 200 mg/kg, a dose that is approximately 50% lower than the LD_{50} previously reported for Swiss Webster male mice (Warren *et al.*, 1982). Subsequent studies exposed mice to NA via inhalation (a predominant route of NA exposure in human population) at an occupationally relevant concentration (10 ppm) (http://www.osha.gov/dts/chemicalsampling/data/CH_255800.html), which also causes airway epithelial injury in mice (Li *et al.*, 2017). Lung-*Cpr*-null mice and their $Cpr^{+/+}$ control littermates were compared for toxicokinetic profiles of plasma NA and NA-glutathione (GSH) conjugates; nonspecific markers of airway cell injury in bronchoalveolar lavage fluid (BALF); and extent of tissue injury and postinjury cellular proliferation in airway epithelia. The results of these studies provide further, more direct data for a dominant role of lung CYP enzymes in NA-induced airway toxicity in mice.

MATERIALS AND METHODS

Chemicals and reagents. NA (CAS No. 91-20-3, purity 99%), NA-d_8 (CAS No. 1146-65-2, purity 99%), GSH (CAS No. 70-18-8, purity ≥ 98.0%), and β-nicotinamide adenine dinucleotide phosphate, reduced tetra(cyclohexyl ammonium) salt (NADPH) (CAS No. 100929-71-3, purity ≥ 95.0%), were purchased from Sigma Aldrich (St Louis, Missouri). Acetaminophen-glutathione (AP-GSH) was purchased from Toronto Research Chemicals (Toronto, Ontario, Canada). NA-GSH standard as a mixture of all 4 stereoisomers was a generous gift from Dr Alan R. Buckpitt and Dr Dexter Morin (University of California at Davis, Davis, California) and was prepared as previously described (Richieri and Buckpitt, 1987). 5-Bromo-2′-deoxyuridine (BrdU) was obtained from Sigma-Aldrich Company (Milwaukee, Wisconsin). All solvents (dichloromethane, formic acid, methanol, and water) were of analytical grade (Fisher Scientific, Houston, Texas).

Mouse breeding and doxycycline treatment. All animal use protocols were approved by the Institutional Animal Care and Use Committee of the Wadsworth Center and University of Arizona Animal Care and Use Committee. The lung-*Cpr*-null mouse was previously generated on the A/J genetic background and utilized to demonstrate the essential role of lung P450-mediated bioactivation in the lung tumorogenesis induced by the tobacco-specific procarcinogen NNK [4-(methylnitrosamino)-1-(3-pyridyl)-1-butanone] (Weng *et al.*, 2007). In this mouse model (CCSP-rtTA$^{+/-}$/tetO-Cre$^{+/-}$/Cpr$^{lox/lox}$), Cpr expression was abolished in many of the airway epithelial Club cells in a doxycycline (DOX) inducible manner. Here, we have recreated the lung-*Cpr*-null mouse model on the C57BL/6 genetic background; the breeding strategy was essentially the same as previously described (Weng *et al.*, 2007), but with minor modifications in the source and genetic background of the CCSP-rtTA$^{+/-}$ and tetO-Cre$^{+/-}$ parental mouse stains used. A graphic representation of the parental strains utilized, breeding scheme, and genetic manipulation is shown in Supplementary Figures 1A and 1B. The Cpr$^{lox/lox}$ (Wu *et al.*, 2003) mice (congenic on C57BL/6) were obtained from breeding stock maintained at Wadsworth Center; CCSP-rtTA$^{+/-}$ (B6.Cg-Tg[Scgb1a1-rtTA]1Jaw/J, catalog No. 006232) and tetO-Cre$^{+/-}$ (B6.Cg-Tg[tetO-cre]1Jaw/J, catalog No. 006234) mice were purchased from Jackson Laboratory (Bar Harbor, Maine). The loxP sites in the *Cpr* gene and the CCSP-rtTA and tetO-Cre transgenes were detected by PCR using tail DNA. The list of PCR primers for, and representative results of, the genotyped alleles is presented in Supplementary Table 1 and Figure 1C, respectively. A 1-kb-plus DNA ladder (Invitrogen, Waltham, Massachusetts) was used for size determination of PCR products. Inducible deletion of the *Cpr* gene in the lung-*Cpr*-null (CCSP-rt-TA$^{+/-}$/tetO-Cre$^{+/-}$/Cpr$^{lox/lox}$) mice was initiated by feeding doxycycline, added to a standard chow diet (625 mg/mg; Envigo Teklad Diets, Madison, Wisconsin; catalog No. TD.02503), starting from E0 (1st day of pairing the parental breeders) until the age of 2 months, according to a previously reported protocol (Hokuto *et al.*, 2004).

Immunofluorescence analysis. All immunofluorescence analyses were performed on approximately 5-μm paraffin sections of formalin-fixed lung tissue. Antigens were retrieved by incubating the slides in Tris-EDTA buffer (10 mM Tris-HCl, 1 mM EDTA,

pH 9.0) for 40 min in a 96°C water bath. After cooling to room temperature and washing with 1× phosphate-buffered saline (137 mM NaCl, 2.7 mM KCl, 10 mM Na_2HPO_4, 1.8 mM KH_2PO_4) the slides were incubated with a mixture of 10% normal goat serum (Invitrogen) and 1% bovine serum albumin (Sigma-Aldrich) in 1× PBS for 1 h at room temperature to block nonspecific binding of the antibodies.

For colocalization of CPR and CCSP, slides were incubated sequentially with a rabbit anti-CPR polyclonal antibody (1:500 dilution, Abcam) in a humidified chamber overnight at 4°C, Alexa-Fluor488-conjugated goat anti-rabbit IgG antibody (1:200 dilution, Abcam) at room temperature for 1 h, the blocking solution for 1 h at room temperature, a rabbit polyclonal anti-uteroglobin (CCSP) antibody (1:1500 dilution, Abcam) for 1 h at room temperature, and Alexa-Fluor594-conjugated goat anti-rabbit IgG antibody (1:200 dilution, Abcam) for 1 h at room temperature, with washing after each antibody incubation step. The slides were then incubated with DAPI to stain nuclei, mounted in a VectorShield antifade medium (Vector Laboratories, Burlington, California), protected with a coverslip, and stored in the dark at 4°C until viewing. For negative controls, the slides were untreated or incubated with a normal goat serum instead of primary antibodies.

Fluorescence images were obtained using a Nikon 50i microscope (Nikon, Melville, New York) at the Wadsworth Center Advanced Light Microscopy Core. The images were captured with a Spot CCD camera (Diagnostic Imaging, Sterling Heights, Michigan) separately using Quad-Fluor filter settings B-2E/C for Alexa Fluor488, UV-2E/C for Alexa Fluor594 and G-2E/C for DAPI to prevent bleed-through effects. The images were imported into the ImageJ program (https://imagej.nih.gov/ij/) where the separate red, green, and blue images were merged and labeled.

The quantification of CPR-positive cells in proximal and distal airways was performed by separately counting cells with green (Alexa Fluor488-positive) signal in the cytoplasm and cells with blue (DAPI-positive) signal in the nuclei. A total of 9 or 10 randomly selected microscopic fields were examined for each mouse; the total number of CPR-positive cells was normalized by the total number of DAPI-positive cells in the examined fields for calculation of the abundance (expressed in percentage) of CPR-positive cells in the airways.

To evaluate the extent of CPR deletion in Club cells, epithelial cells in different airway regions that were positive for both CPR and CCSP, as well as all cells that were positive for CCSP, were separately counted. The total number of double-positive cells (CPR^+ and $CCSP^+$) in 4 or 5 randomly selected microscopic fields was counted per mouse, normalized to total number of CCSP-positive cells, and expressed as a percentage of the whole.

Animal experiments. Two- to 3-month-old male lung-*Cpr*-null mice and their control littermates (Supplementary Figure 1A) ($n = 3$–4 per group), all on the doxycycline-enriched diet, were used for the study. Males were used in this study for consistency with previously published results (Kovalchuk *et al.*, 2017; Li *et al.*, 2017). The mice either received a single intraperitoneal injection of 200 mg/kg NA in corn oil, or corn oil alone, or were nose-only exposed in a single 4-h session to 10-ppm NA in HEPA-filtered air (FA), or FA alone (sham-exposure control) in an Oral Nasal Aerosol Respiratory Exposure System (CH Technologies, Westwood, New Jersey) as previously described (Kovalchuk *et al.*, 2017). NA vapor, generated by passing air through a glass column containing crystalline NA, heated to 52°C, was diluted with fresh FA to achieve desired average NA concentration in the inhalation chamber. NA vapor at 10-ppm concentration is an OSHA permissible exposure limit for human workers (http://www.osha.gov/dts/chemicalsampling/data/CH_255800.html). The 4-h total exposure time was selected to mimic daily occupational exposure. A model IQ-604 Total Volatile Organic Compound (TVOC) Monitor (Graywolf Sensing Solutions, Trumbull, Connecticut), precalibrated for NA, was used to monitor real-time concentrations of NA, carbon dioxide (CO_2), carbon monoxide (CO), and oxygen (O_2); relative humidity; and air temperature in the exposure chamber throughout the exposure session.

For toxicokinetic studies, blood samples (approximately 20 µl each) from individual mice were collected from the tail vein using heparin-coated capillary tubes at various time points (0–600 min) after termination of NA administration. Plasma was prepared by centrifugation of blood samples at 10 000 rpm in an Eppendorf 5424R centrifuge for 8 min at 4°C, and was stored in sealed tubes at −80°C until use.

For acute toxicity studies, these same mice were euthanized using carbon dioxide 20 h after termination of the 4-h inhalation NA exposure session, or 24 h after the single intraperitoneal injection of NA at 200 mg/kg. The trachea was exposed; a cannula was inserted and tied in place to collect BALF. BALF was obtained by lavaging the lung once with 1 ml of calcium- and magnesium-free, prewarmed, PBS, at pH 7.1. The cells in BALF were pelleted by centrifugation at 1600 rpm for 5 min in an Eppendorf 5424R centrifuge. A portion of the cell-free BALF was immediately used to measure lactate dehydrogenase (LDH) activity with CytoTox 96 Non-Radioactive Cytotoxicity Assay (Promega, Madison, Wisconsin), performed according to the manufacturer's instructions. The amount of protein in BALF was determined by the Pierce bicinchoninic acid assay (Thermo Scientific, Waltham, Massachusetts) using bovine serum albumin as the standard.

For histopathologic examination, the lungs were perfusion-fixed via the trachea with 10% neutral buffered formalin at a constant pressure of 20–25 cm of fixative. After a minimum of 1-h fixation, the trachea was ligated and the fully inflated lung was placed in a large volume of the same fixative, and then embedded in paraffin. Tissue sections (5 µm thick) were stained with hematoxylin and eosin. The incidence of lesioned airways was scored in 5 randomly selected microscopic fields per lung section at ×200 magnification (as a percentage of the total number of airways examined; 2 slides per mouse) and compared among groups in a blinded fashion.

For identification of proliferating cells, a separate set of mice were euthanized at 48 h after either the initiation of the 4-h NA inhalation exposure session, or the administration of the single intraperitoneal NA injection, and all mice were also injected with BrdU (at 50 mg/kg in 1× PBS) 1 h prior to death. All lungs were perfusion-fixed as described above. The small intestine of BrdU-treated mice (used as a positive control during pilot studies for BrdU detection) was also collected, fixed in 10% neutral buffered formalin for 24 h, and paraffin-embedded.

Immunohistochemistry. For BrdU detection, unstained sections (approximately 5 µm thick) of mouse lung were evaluated using immunohistochemistry. Antigen retrieval was performed as described (Lawson *et al.*, 2002; Van Winkle *et al.*, 1995). In brief, deparaffinized and rehydrated lung sections were digested in 2N hydrochloric acid at 60°C for 15 min and then neutralized in 0.1-M sodium borate buffer, pH 9.0, for 10 min. Sections were exposed to 0.05% proteinase (in TE buffer, pH 8.0) at 37°C for 10 min followed by blocking with 3% hydrogen peroxide in methanol. The lung sections were then incubated sequentially

with biotin-labeled, prediluted anti-BrdU (Abcam) at a 1:2 further dilution in 1× PBS, for 2 h, and a streptavidin-horse radish peroxidase-conjugate (Abcam) for 10 min, at room temperature. Antigen-antibody complexes were visualized with 3,3′-diaminobenzidine as the substrate. Negative control sections were either from mice not treated with BrdU, or from BrdU-treated animals, but incubated with 1× PBS in place of the primary antibodies. Sections of small intestine of BrdU-treated animals were used as a positive control.

The number of cells with BrdU-labeled nuclei was counted digitally, using either a Nikon 50i light microscope equipped with a digital camera or a Leica DMI6000B microscope equipped with a DFC450 color digital camera that is linked to a computer running the LAS X version 3.3 software (Leica Microsystems., Buffalo Grove, Illinois). Cells with dark nuclear staining were considered as positive and the numbers were counted in airways in 5 randomly selected microscopic fields per lung section, at ×200 magnification. BrdU labeling index (LI) was determined by dividing the number of BrdU-positive cells by the total number of epithelial cells (sum of BrdU-positive and -negative cells) and multiplying by 100% (Hotchkiss *et al.*, 1997). Data are presented as means ± SD of 3–4 mice per group.

Detection and quantification of NA and NA-GSH. NA was measured in mouse plasma using an Agilent 7890A gas chromatograph with automated liquid sampler and coupled to an Agilent 5975C inert XL EI/CI mass spectrometer (Agilent, Santa Clara, California). Each plasma sample (10 µl) was spiked with an internal standard NA-d_8 (8 ng in 10 µl of methanol) (Sigma-Aldrich) and extracted with 100 µl of dichloromethane as described previously (Kovalchuk *et al.*, 2017). The organic phase was collected and 1 µl was injected using splitless injection mode. The analytes were separated on a Restek Rxi-5ms (30 m × 0.25 mm; 0.25 µm) column (Restek, Bellefonte, Pennsylvania) under a constant flow (1 ml/min) of helium. Analytes detection was done using selected ion monitoring at 128.0 *m/z* for NA, and 136.0 *m/z* for NA-d_8. Blank plasma from naïve mice was spiked with freshly prepared NA standards (2–5000 ng/ml) and NA-d_8 to create a calibration curve for quantifying NA in plasma samples. The lower limit of quantification (signal-to-noise ratio > 10) for NA was 0.04 pmol on column; the analyte recovery was > 90% at all concentrations tested.

NA-GSH was detected as previously described (Kovalchuk *et al.*, 2017) using an AB SCIEX 6500+ QTRAP triple quadrupole linear ion trap mass spectrometer (AB SCIEX, Framingham, Massachusetts) coupled to an Agilent 1290 Infinity series

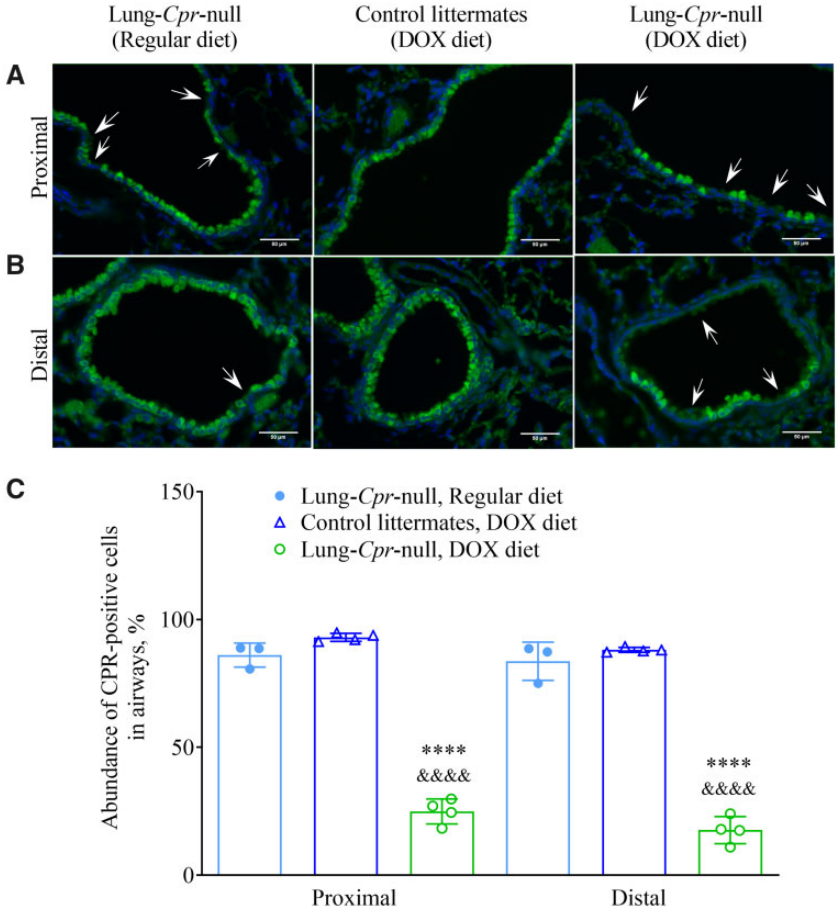

Figure 1. Efficiency of *Cpr* gene deletion in airway epithelial cells. Lung sections were obtained from naïve 2-month old males and stained with antibodies against CPR (green) followed by nuclear counterstaining with DAPI (blue). Representative images are shown for proximal (A) and distal (B) airways from lung-*Cpr*-null (CCSP-rtTA$^{+/-}$/tetO-Cre$^{+/-}$/Cpr$^{lox/lox}$)/regular diet, lung-*Cpr*-null/doxycycline-containing diet (DOX diet), and control littermates (CCSP-rtTA$^{+/-}$/Cpr$^{lox/lox}$ or tetO-Cre$^{+/-}$/Cpr$^{lox/lox}$)/DOX diet groups. Arrows point to regions with loss of CPR-positive epithelial cells in airways. The scale bar is 50 µm. C, Abundance of CPR-positive epithelial cells in proximal and distal airways. The total number of CPR-positive epithelial cells was counted in 9 or 10 randomly selected microscopic fields per mouse (at ×200) and normalized by the total number of DAPI-positive cells. The values are presented as means ± SD (3–4 mice in each group). $^{****}p < .0001$ compared with lung-*Cpr*-null/regular diet; $^{\&\&\&\&}p < .0001$, compared with control littermates/DOX diet (2-way ANOVA followed by Bonferroni's test for multiple comparisons).

ultra-high-performance liquid chromatography system. Each plasma sample (10 µl) was diluted with 10% UPLC-MS grade methanol and spiked with an internal standard AP-GSH (3.75 ng in 10 µl of methanol). Samples were centrifuged at 14 000 rpm for 10 min in an Eppendorf 5424R centrifuge to precipitate proteins; the supernatant was collected and processed using IsoluteC18 25-mg/1-ml solid phase extraction (SPE) cartridges (Biotage, Charlotte, North Carolina). Samples were applied to the SPE cartridge in 10% methanol; the unbound fraction and an additional wash with 1 ml of 10% methanol were collected and used for UPLC-MS analysis. Chromatographic separation and MS detection of NA-GSH and AP-GSH were done as described recently (Kovalchuk *et al.*, 2019). Five-point calibration curves were constructed by adding the internal standard and authentic standard (5–1500 ng/ml) to the plasma from naïve mice. The lower limit of quantification (signal-to-noise ratio > 10) for NA-GSH was 0.02 pmol on column; the analyte recovery during SPE was approximately 75%.

Other methods. Data from multiple groups were compared using 2-way ANOVA, followed by Bonferroni post hoc test for pairwise comparisons, using GraphPad Prism (GraphPad, La Jolla, California). A p value less than .05 was considered to be statistically significant.

RESULTS

Characterization of the Lung-Cpr-Null Mice

The newly generated lung-*Cpr*-null mice on the C57BL/6 genetic background, on either DOX-containing diet or regular chow diet, were normal compared with their control littermates, in gross morphological features, development, and fertility. Body and organ weights (lung, liver, and kidney) were similar between lung-*Cpr*-null mice and their control littermates. As expected, genotype frequency among pups from doxycycline-treated breeders (CCSP-rtTA$^{+/-}$/Cpr$^{lox/lox}$ × tetO-Cre$^{+/-}$/Cpr$^{lox/lox}$; Supplementary Figure 1) was 27% for CCSP-rtTA$^{+/-}$/tetO-Cre$^{+/-}$/Cpr$^{lox/lox}$ (29/108), 26% for CCSP-rtTA$^{+/-}$/tetO-Cre$^{-/-}$/Cpr$^{lox/lox}$ (28/108), 24% for CCSP-rtTA$^{-/-}$/tetO-Cre$^{-/-}$/Cpr$^{lox/lox}$ (26/108), and 23% for

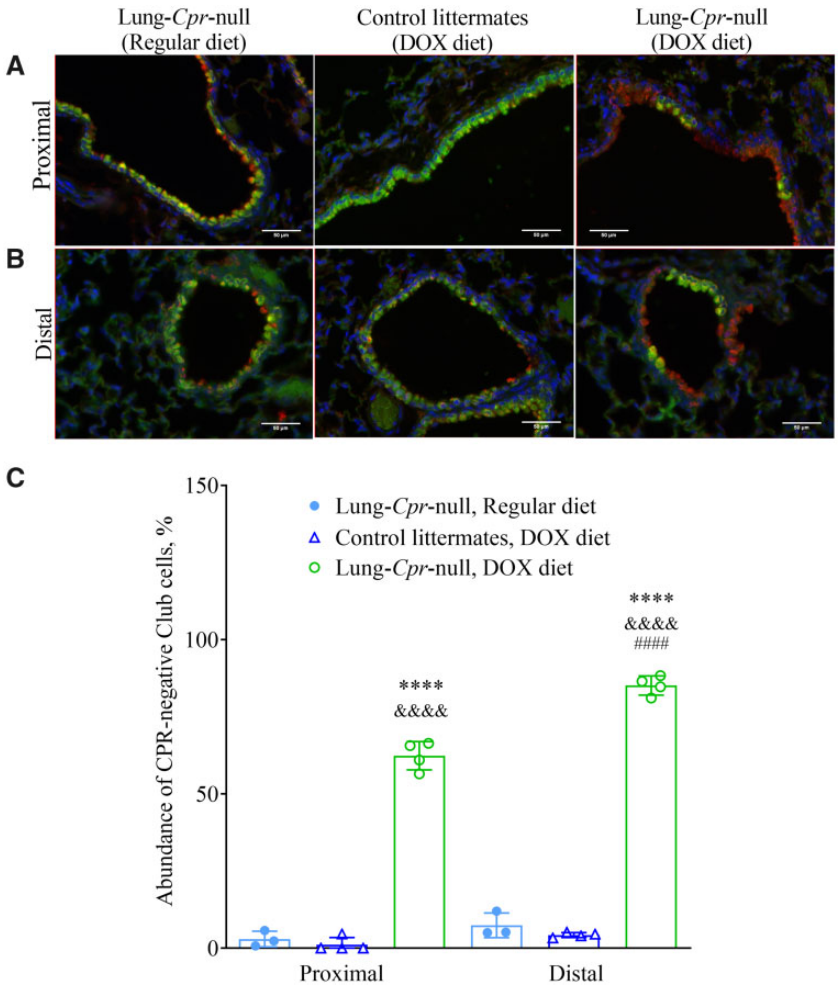

Figure 2. Targeted deletion of CPR in airway epithelial Club cells. Lung sections obtained from naïve 2-month-old male mice were stained with antibodies against CPR (green) and CCSP (red), followed by nuclear counterstaining with DAPI (blue). Representative images are shown for proximal (A) and distal (B) airways. The scale bar is 50 µm. C, Abundance of CPR-negative Club cells in proximal and distal airways. The total number of CPR-negative Club cells was counted in 4 or 5 randomly selected microscopic fields per mouse (at ×200) and normalized by the total number of CCSP-positive cells. The values are presented as means ± SD (3–4 mice in each group). $^{****}p < .0001$ compared with lung-*Cpr*-null/regular diet; $^{\&\&\&\&}p < .0001$, compared with control littermates/DOX (doxycycline) diet; $^{\#\#\#\#}p < .0001$, compared with proximal airways of the lung-*Cpr*-null/DOX diet group (2-way ANOVA followed by Bonferroni's test for multiple comparisons).

CCSP-rtTA$^{-/-}$/tetO-Cre$^{+/-}$/Cpr$^{lox/lox}$ (25/108) mice ($p > .05$, χ^2 test), suggesting absence of embryonic lethality.

DOX-induced deletion of the *Cpr* gene in lung-*Cpr*-null mice was demonstrated by immunohistochemical determination and quantification of CPR-positive and -negative epithelial cells in proximal and distal airways (Figure 1). In contrast to control littermates on DOX-containing diet, in which nearly all epithelial cells were positive for CPR expression (93% in proximal airways and 88% in distal airways), lung-*Cpr*-null mice on DOX-containing diet had only 25% (proximal)-18% (distal) CPR-positive cells remaining at 2 months of age (Figure 1C). Notably, the detection of a slightly smaller number of CPR-positive airway epithelial cells in lung-*Cpr*-null mice on regular chow (89% and 84%, respectively, for proximal and distal airways), than in control littermates on DOX-containing diet, was as expected, based on the known "leakiness" of the tetO-Cre transgene expression (Perl *et al.*, 2002, 2005; Weng *et al.*, 2007).

The extent of *Cpr* gene deletion in the main target cells of NA toxicity, the airway Club cells, was determined by immunohistochemical detection of CPR-positive and -negative Club cells, which are CCSP-positive (Figure 2). The relative abundance of CPR$^-$/CCSP$^+$ cells, compared with all CCSP$^+$ cells, in the proximal and distal airways was 62.4% and 85.2%, respectively, in DOX-treated lung-*Cpr*-null mice (Figure 2C). In contrast, only a small number of CPR$^-$/CCSP$^+$ cells were detected in the airways of the control mice. The images of negative controls are presented in Supplementary Figure 2.

Pharmacokinetic Profiles of Plasma NA and NA-GSH in Lung-Cpr-Null Mice and Control Littermates

Plasma levels of NA and NA-GSH were measured in lung-*Cpr*-null mice and their control littermates (both on DOX-containing diet) following a single 4-h inhalation exposure session (Figs. 3A and 3B) or a single intraperitoneal injection of 200 mg/kg NA (Figs. 3C and 3D). Pharmacokinetic profiles for plasma NA and NA-GSH were not different between lung-*Cpr*-null mice and their control littermates irrespective of the route of NA administration, though the maximum levels of plasma NA (at 30 min) and NA-GSH (at 2 h) in mice treated with NA intraperitoneally (at 200 mg/kg; 2.5–2.7 μg NA/ml and approximately 1.0 μg NA-GSH/ml) were much higher than the maximum plasma NA and NA-GSH levels in mice exposed to NA via inhalation (at 10 ppm; 65–99 ng NA/ml and 29 ng NA-GSH/ml), measured immediately after the termination of active exposure. The plasma NA concentration in the intraperitoneal administration group was similar to previously published data, obtained at the same NA dose (Hu *et al.*, 2014), which validated the NA dose accuracy in this study. These results confirm that the loss of CPR expression in airway epithelial cells did not impact systemic clearance of inhaled or intraperitoneally injected NA.

NA-induced Acute Cytotoxicity in the Airway Epithelium of Lung-Cpr-Null Mice and Control Littermates

The total protein concentration and LDH activity in BALF were measured as indicators of acute cytotoxicity in airways, in mice exposed to NA via inhalation. As shown in Figure 4A, NA exposure caused an increase in LDH activity (approximately 2-fold; 95% confidence interval, 1.8- to 2.5-fold) in cell-free BALF from control littermates but not in BALF from lung-*Cpr*-null mice. NA inhalation exposure led to a substantial increase in the total protein concentration in cell-free BALF in both lung-*Cpr*-null mice and control littermates; however, the extent of increase was greater in control littermates (6.5-fold; 95% confidence interval, 5.2- to 7.9-fold) than in lung-*Cpr*-null mice (4.2-fold; 95%

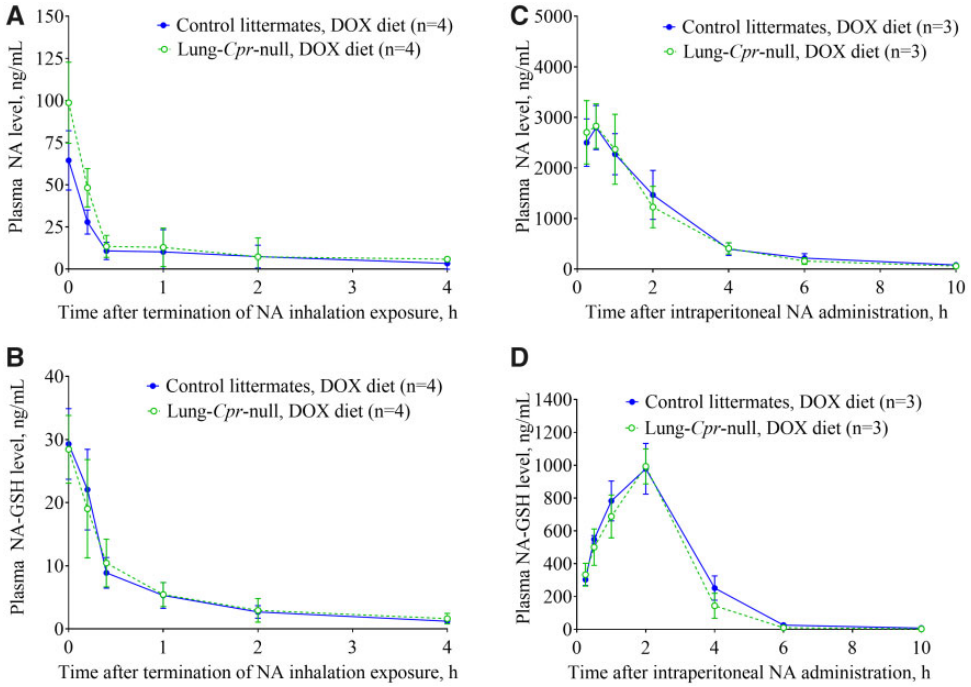

Figure 3. NA (naphthalene) and NA-GSH levels in the plasma following NA exposure. Two- to 3-month-old male lung-*Cpr*-null mice and their control littermates, both on doxycycline (DOX)-containing diets, were exposed to 10-ppm NA in a single 4-h inhalation session or received a single intraperitoneal injection of 200-mg/kg NA. NA and NA-GSH levels were determined in plasma obtained from individual mice at various time intervals after termination of NA inhalation exposure (A, B) or after NA injection (C, D), as described in the Materials and Methods section. Data represent means ± SD ($n = 3$–4). A significant genotype-related difference was not found ($p > .05$) at any time-point examined, for either NA or NA-GSH.

confidence interval, 3.1- to 5.4-fold), compared with genotype-matched FA controls (Figure 4B). The difference in fold increase between the control littermates and lung-*Cpr*-null mice (by approximately 60%) was statistically significant ($p < .0001$). Together, these results provide evidence of the important role of local CYP-mediated bioactivation of inhaled NA in inducing acute cytotoxic airway epithelial injury.

The extent of acute airway damage was compared between lung-*Cpr*-null and control littermates following different routes of NA administration (Figs. 5 and 6). The incidence of lesioned airways varied by mouse genotype and administration route. The incidences were approximately 2-fold lower in both proximal and distal airways of lung-*Cpr*-null mice than in control littermates, following either intraperitoneal NA injection (Figs. 5C and 5D) or 10-ppm NA inhalation (Figs. 6C and 6D). However, the incidences of airway lesions were significantly lower after NA inhalation exposure than after intraperitoneal administration, for either genotype (by approximately 3-fold). The incidence of lesions was less than 20% in lung-*Cpr*-null mice following NA inhalation exposure.

In control littermates, the severity of acute intrapulmonary airway cytotoxicity varied by the 2 different treatment protocols; signs of tissue injury in the control littermates, including perturbation of epithelial lining (swollen cells and attenuated epithelial thickness) and detachment of epithelial cells from basal membrane in both proximal and distal airways, were most evident following an intraperitoneal injection of 200 mg/kg NA (Figure 5), though also detected after an inhalation exposure session at 10-ppm NA (Figure 6). With either route, the acute cytotoxicity in airways of lung-*Cpr*-null mice was confined to the airway epithelium.

Proliferative Response to NA-induced Airway Epithelial Injury in Lung-Cpr-Null Mice and Control Littermates

BrdU incorporation into nuclear DNA was detected as a marker of cellular proliferation, examined at 2 days following NA exposure via inhalation or intraperitoneal injection. Initial studies were conducted in mice treated intraperitoneally with NA, and were focused on detecting BrdU-positive cells in the distal airways. As shown in Figure 7a, BrdU-positive cells, which were scarce in vehicle-treated mice (regardless of genotype), were abundant in NA-treated control littermates, but were present in much lower numbers in NA-treated lung-*Cpr*-null mice. The BrdU LI in NA-treated control littermates was 4.3-fold higher than in NA-treated lung-*Cpr*-null mice (Figure 7B). Further studies were conducted in mice exposed to NA via inhalation, and the proliferative response was determined for both proximal and distal airways. As shown in Figures 8A and 8B, in either proximal or distal airways, BrdU-positive epithelial cells were rarely detected in mice (lung-*Cpr*-null or control littermates) exposed to FA, abundant in NA (10 ppm)-exposed control littermates, but present in much lower numbers in NA (10 ppm)-exposed lung-*Cpr*-null mice. BrdU LI in proximal and distal intrapulmonary airways were similar in NA-exposed control littermates (12- to 13-fold higher than the basal level seen in FA groups), or in NA-exposed lung-*Cpr*-null mice (4- to 5-fold higher than in FA groups) (Figs. 8C and 8D). The BrdU LI was 2.4- and 2.9-fold higher, in proximal and distal airways, respectively, in NA-exposed control littermates than in NA-exposed lung-*Cpr*-null mice. Taken together, these findings provide additional evidence to confirm that CYP-mediated NA bioactivation in the lung played an important role in NA-induced cytotoxicity, and the consequent activation of proliferative repair, in the airway epithelium.

DISCUSSION

The lung-*Cpr*-null mouse on the C57BL/6 genetic background used in this study was similar to the one generated previously on the A/J background (Weng *et al.*, 2007). Both models show an absence of any gross biological phenotype, effective ablation of CPR expression in Club cells, and minor leakiness of Cre expression in mice not treated with DOX (Figs. 1 and 2). Notably, the transgenic rat CCSP promoter targets Cre expression and *Cpr* deletion to Club cells in conducting airways as well as type II epithelial cells in the alveoli (Weng *et al.*, 2007). CPR expression level in alveolar epithelial cells is much lower than in Club cells (Figs. 1 and 2). The extent of CPR ablation in the alveoli, which was not examined in this study, was previously estimated, based on PCR analysis of *Cpr* gene deletion, to occur in > 30% of all alveolar type II epithelial cells in the lung-*Cpr*-null mice on A/J background (Weng *et al.*, 2007). The extent of CPR ablation in Club cells, quantified for the first time in this study, seemed to be even greater, at 66% (proximal airways)-86% (distal airways) (Figure 2).

The pharmacokinetic profiles (Figure 3) of plasma NA and NA-GSH were similar between lung-*Cpr*-null mice and control littermates, regardless of the routes of NA exposure. This data confirmed that CYP-mediated NA metabolism in the airway epithelial cells did not significantly contribute to systemic

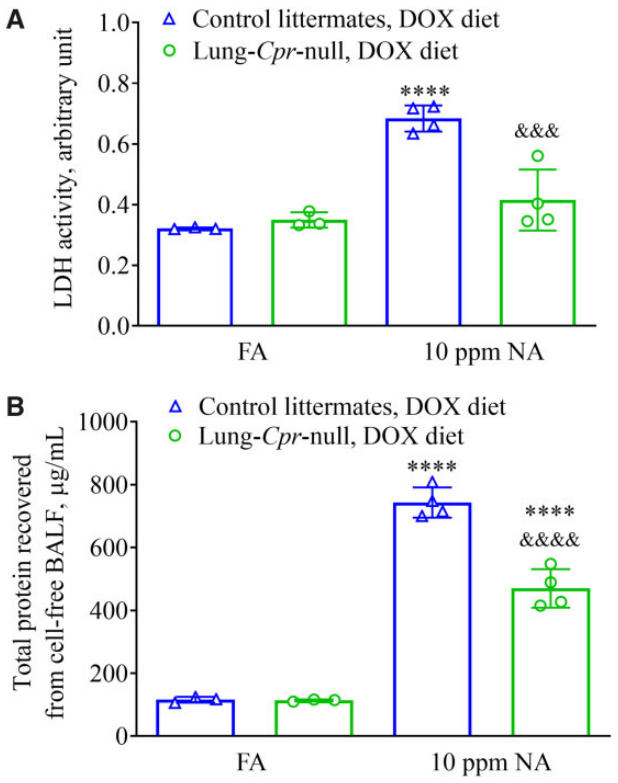

Figure 4. NA (naphthalene) exposure-induced changes in bronchoalveolar lavage fluid (BALF). Two- to 3-month-old lung-*Cpr*-null mice and their control littermates were exposed to either filtered air (FA) or 10-ppm NA for 4 h. The lungs of individual mouse were lavaged 20 h after the termination of inhalation exposure to obtain BALF, as described in the Materials and Methods section. Lactate dehydrogenase (LDH) activity (A) and total protein concentration (B) were measured in BALF as nonspecific markers of cytotoxicity. Data represent means ± SD ($n = 3$–4 per each group). $^{****}p < .0001$, by exposure; $^{\&\&\&}p < .001$, $^{\&\&\&\&}p < .0001$, by genotype (2-way ANOVA followed by Bonferroni's test for multiple comparisons).

clearance of the administered toxicant. The finding agrees with previously published data for pharmacokinetic profiles of NNK and its metabolite NNAL in lung-*Cpr*-null mice and control littermates (Weng *et al.*, 2007). However, more recent studies using CYP2A13/2F1-humanized mice on the *Cyp2abfgs*-null and LCN background (Kovalchuk *et al.*, 2019) showed that, in mice with substantially attenuated ability to metabolize NA (due to selective loss of hepatic microsomal P450 activity and whole body loss of CYP2A, 2B, 2F, 2G, and 2S expression), transgenic expression of human CYP2A13/2F1 in the lungs caused a notable increase in rates of systemic NA clearance. Thus, the pulmonary contribution to systemic NA clearance is negligible in mice with normal levels of hepatic P450 activity, though it could be more substantial in situations where hepatic NA metabolism is severely compromised, which may result from severe liver dysfunction and cirrhosis. Importantly, the lack of a substantial difference in plasma levels of NA or NA-GSH between lung-*Cpr*-null mice and control littermates validates that the observed differences in NA toxicity between these 2 groups were not complicated by differences in systemic NA clearance, as was the case with the LCN mice (Kovalchuk *et al.*, 2017).

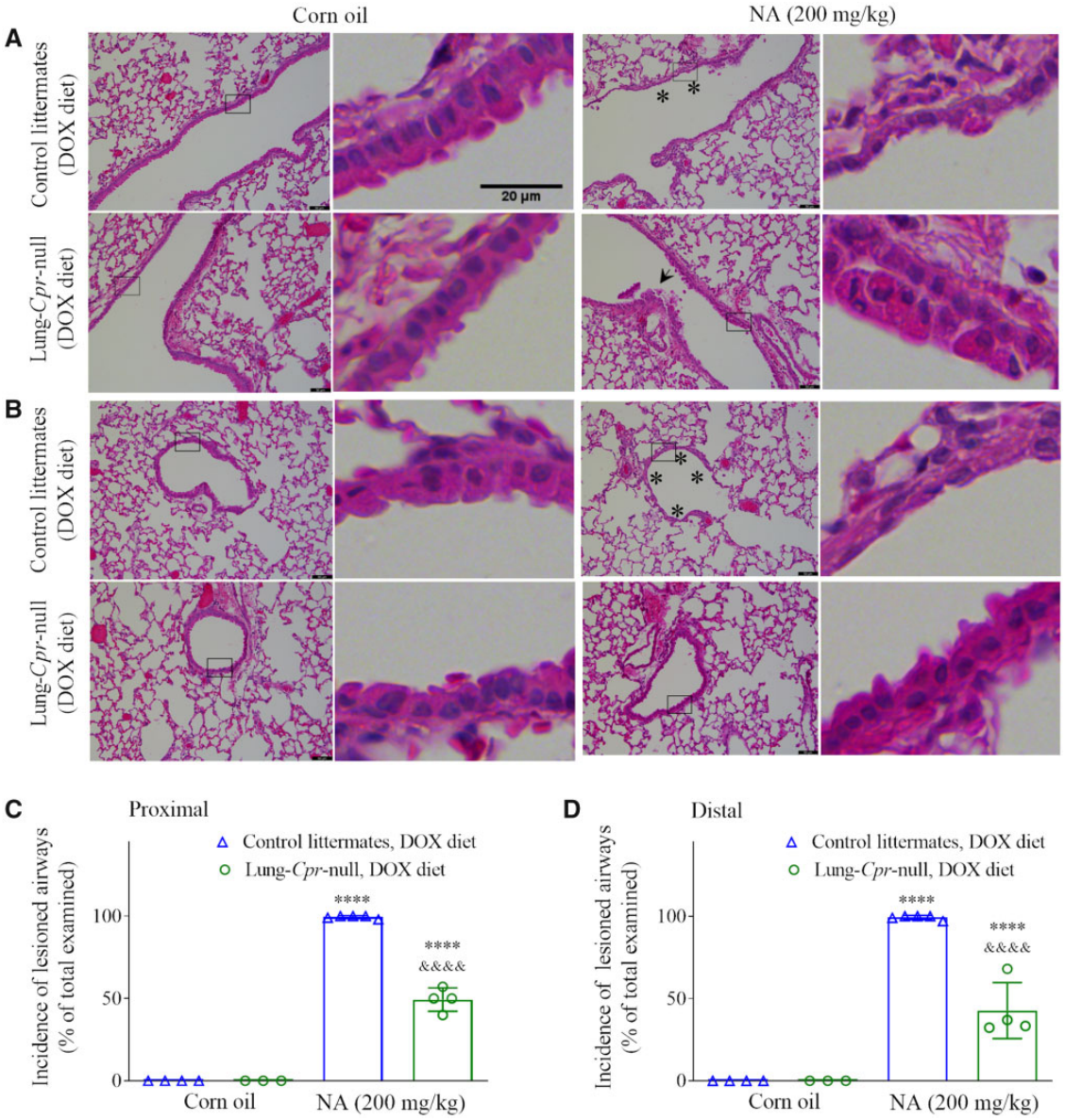

Figure 5. Histopathologic analysis of acute airway damage in lung-*Cpr*-null mice and control littermates following intraperitoneal administration of NA. Two- to 3-month-old lung-*Cpr*-null mice and their control littermates received a single intraperitoneal injection of 200-mg/kg naphthalene (NA) in corn oil or corn oil alone. The lungs were collected 24 h after NA injection. Representative images of hematoxylin and eosin-stained proximal (A) and distal (B) airways (×200 magnification) are shown. Boxed areas in the left panel (Bar is 50 µm) are shown at higher magnification in the right panel (Bar is 20 µm). Vehicle control mice (corn oil) had normal epithelial cells attached to the basal membrane. NA-treated control littermates showed wide-spread detachment of airway epithelia from basement membrane in both proximal and distal airways (asterisks); whereas NA-treated lung-*Cpr*-null mice had only occasional focal damage in the proximal airways (arrow). The incidence (%) of airways with lesions (either detachment or focal damage) was quantified for proximal (C) and distal (D) airways, as described in the Materials and Methods section. Results represent means ± SD ($n = 3$–5 per group). $^{\&\&\&\&}p < .0001$, by mouse genotype; $^{****}p < .0001$, by exposure (2-way ANOVA followed by Bonferroni's test for multiple comparisons). Abbreviation: DOX, doxycycline.

Increases in the concentration of total protein and LDH activity in cell-free BALF serve as nonspecific markers of pulmonary injury (Kristof *et al.*, 1998). Exposure to inhaled NA caused an approximately 2-fold increase in LDH activity and an approximately 6.5-fold increase in total protein concentration in the cell-free BALF of control mice at 24 h after exposure, consistent with occurrence of acute lung cytotoxicity (Figure 4). These increases were abolished (LDH) or attenuated (total protein) in the lung-*Cpr*-null mice, which provided evidence for an important role of lung airway epithelial CPR/P450 enzymes in mediating NA's acute cytotoxicity. In the lung-*Cpr*-null mice, NA exposure still caused lung toxicity, as indicated by the approximately 4-fold increase in cell-free BALF protein concentration (which indicates vascular leakage as well as airway cell damage), compared with FA-exposed mice. This residual toxicity may be explained by NA bioactivation in lung cells that still express CPR and by toxic effects of NA reactive metabolites derived from systemic circulation. In that regard, the apparent absence of an increase in cell-free BALF LDH (which indicates airway cell damage or death) in NA-exposed lung-*Cpr*-null mice may reflect a greater effect of circulating (than locally produced) toxic NA metabolites on the lung vasculature, an idea that warrants further investigation.

Club cells serve not only as sites of metabolic activation of toxicant within the lung but they serve also as progenitor cells for postinjury tissue repair. BrdU incorporation in airway

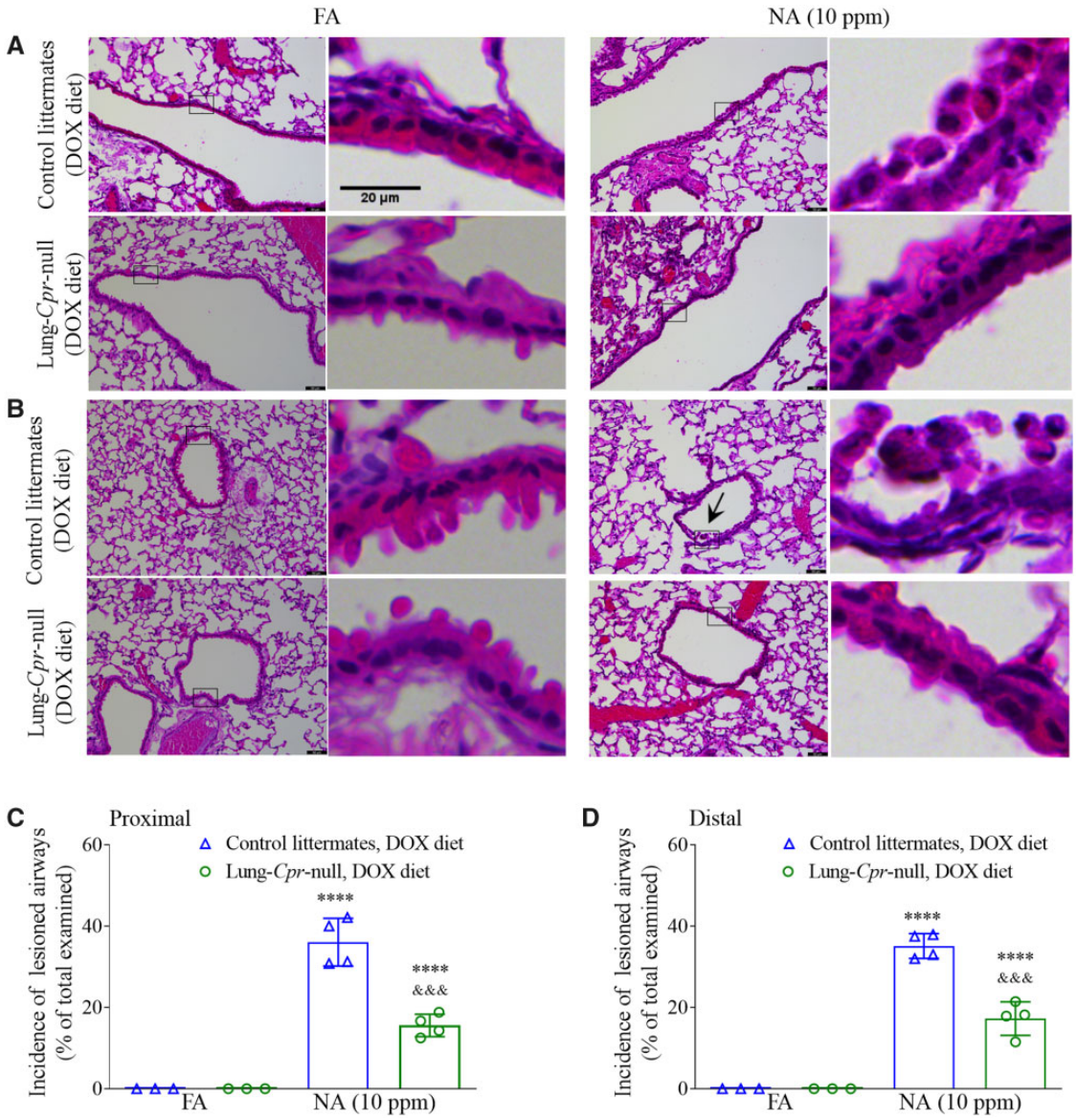

Figure 6. Histopathologic analysis of acute airway damage in lung-*Cpr*-null mice and control littermates following inhalation exposure to naphthalene (NA). Two- to 3-month-old lung-*Cpr*-null mice and their control littermates were exposed via inhalation to either filtered air (FA) or 10-ppm NA for 4 h. The lungs were collected 20 h after NA inhalation exposure. Representative images of hematoxylin and eosin-stained proximal (A) and distal (B) airways (×200 magnification) are shown. Boxed areas in the left panel (Bar is 50 µm) are shown at higher magnification in the right panel (Bar is 20 µm). None of the animals showed obvious epithelial injury. Occasional focal damage was seen in the distal airways of NA-treated control littermates (arrow). The incidence (%) of airways with lesions (focal damage) was quantified for proximal (C) and distal (D) airways, as described in the Materials and Methods section. Results represent means ± SD ($n = 3$–4 per group). $^{\&\&\&}p < .001$, by mouse genotype; $^{****}p < .0001$, by exposure (2-way ANOVA followed by Bonferroni's test for multiple comparisons). Abbreviation: DOX, doxycycline.

epithelial cells is another measure of Club cell injury and replacement. Similar to the results from BALF protein analysis, the number of proliferating, BrdU-positive cells in airways of NA-treated lung-*Cpr*-null mice was lower than in NA-exposed control mice, at 2 days after NA exposure, but still greater than in vehicle-treated groups, regardless of the route of exposure (Figs. 7 and 8). Thus, toxic metabolites of inhaled or systemically administered NA, generated locally in airway epithelial cells by CYP enzymes, greatly contributed to NA-induced airway epithelial injury; whereas systemically derived NA metabolites may be at least partly responsible for the epithelial damage seen in the NA-exposed lung-*Cpr*-null mice. Notably, although females were not included in this study, we believe that this system level metabolic mechanism applies to both males and females, a notion to be confirmed in future studies.

The internal, circulating levels of NA potentially available for CYP-mediated bioactivation differed substantially in the 2 different NA exposure models, with maximum plasma concentration being approximately 30 times higher in the intraperitoneal injection model than in the inhalation exposure model (Figure 3). Yet the degree of airway epithelial injury induced by NA exposure in the control littermates, judging from the BrdU labeling indices in the distal airways, were comparable between the 2 exposure routes (both were approximately 20%). Although there are possible exposure route-related differences in the extent of injury in Figures 5 and 6 (exfoliation more evident in the intraperitoneal groups compared with inhalation groups), NA exposure via inhalation (over 4 h) appears to be more efficient in stimulating airway cell proliferation. These observations suggest greater overall (extrapulmonary and intrapulmonary) airway epithelial injury in the group exposed by inhalation compared with the group exposed by bolus intraperitoneal injection. In that regard, impacts of NA inhalation on proximal extrapulmonary airways have been reported previously (Boland *et al.*, 2004); whereas NA intraperitoneal injection is known to influence the most distal airways first, with injuries increasing in a proximal direction with increasing dose (Plopper *et al.*, 1992b).

In conclusion, the results of this study directly validate the notion that microsomal CYP enzymes in airway epithelial cells play a large role in causing injury to airway epithelia following exposure to NA via either the inhalation or intraperitoneal route, as well as provide further support to the likely contribution of systemically derived NA metabolites in NA-induced airway injury. These findings are important for assessing the toxic risks from environmental or occupational exposure to NA in humans.

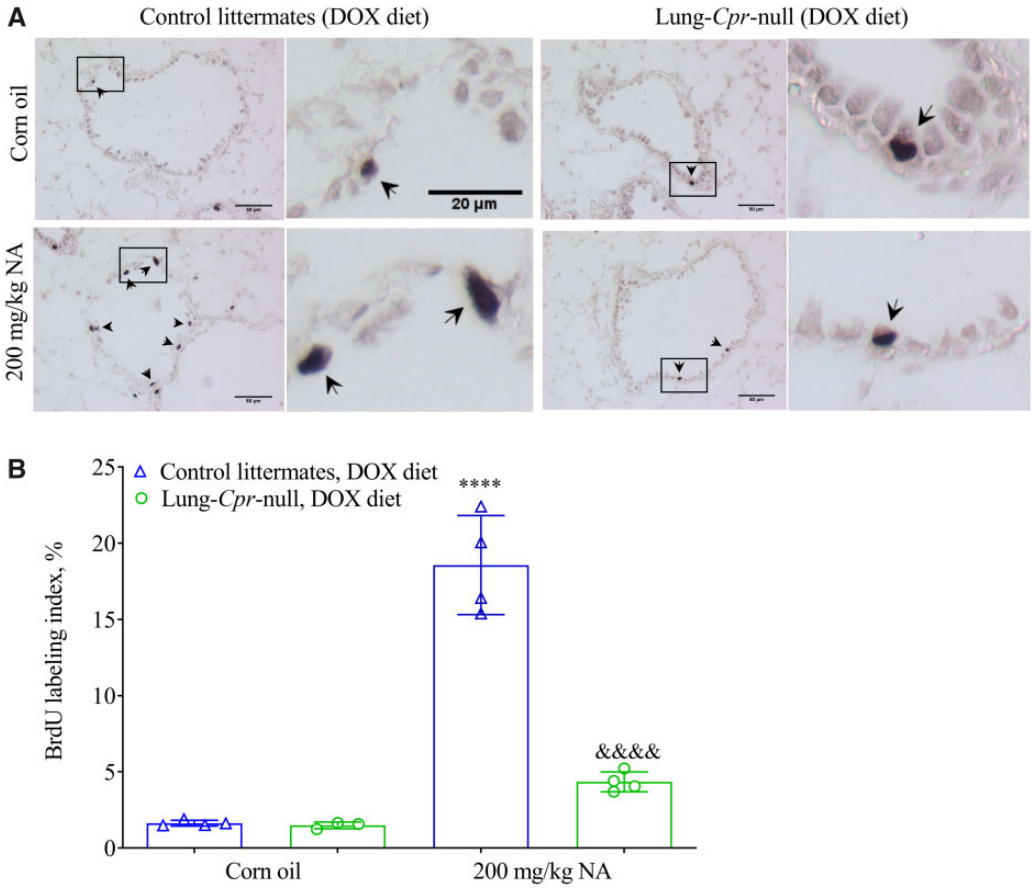

Figure 7. BrdU (5-bromo-2′-deoxyuridine) labeling index in airway epithelial cells after naphthalene (NA) exposure via intraperitoneal injection. Two- to 3-month-old lung-*Cpr*-null mice and their control littermates received a single intraperitoneal injection of 200-mg/kg NA or corn oil. Lungs were collected 2 days after the treatment and immunohistochemically stained for nuclear incorporation of BrdU. Representative images of BrdU-positive cells in distal airways (A) are shown (arrows point to dark-labeled nuclei located in airway epithelium). Boxed areas in the left panel (Bar is 50 μm) are shown at higher magnification in the right panel (Bar is 20 μm). The proportion (%) of BrdU-positive cells was quantified (B) as described in the Materials and Methods section. Results represent means ± SD ($n = 3$–4 mice). $^{\&\&\&\&}p < .0001$, by mouse genotype in the same exposure group; $^{****}p < .0001$, by exposure (2-way ANOVA followed by Bonferroni's test for multiple comparisons). Abbreviation: DOX, doxycycline.

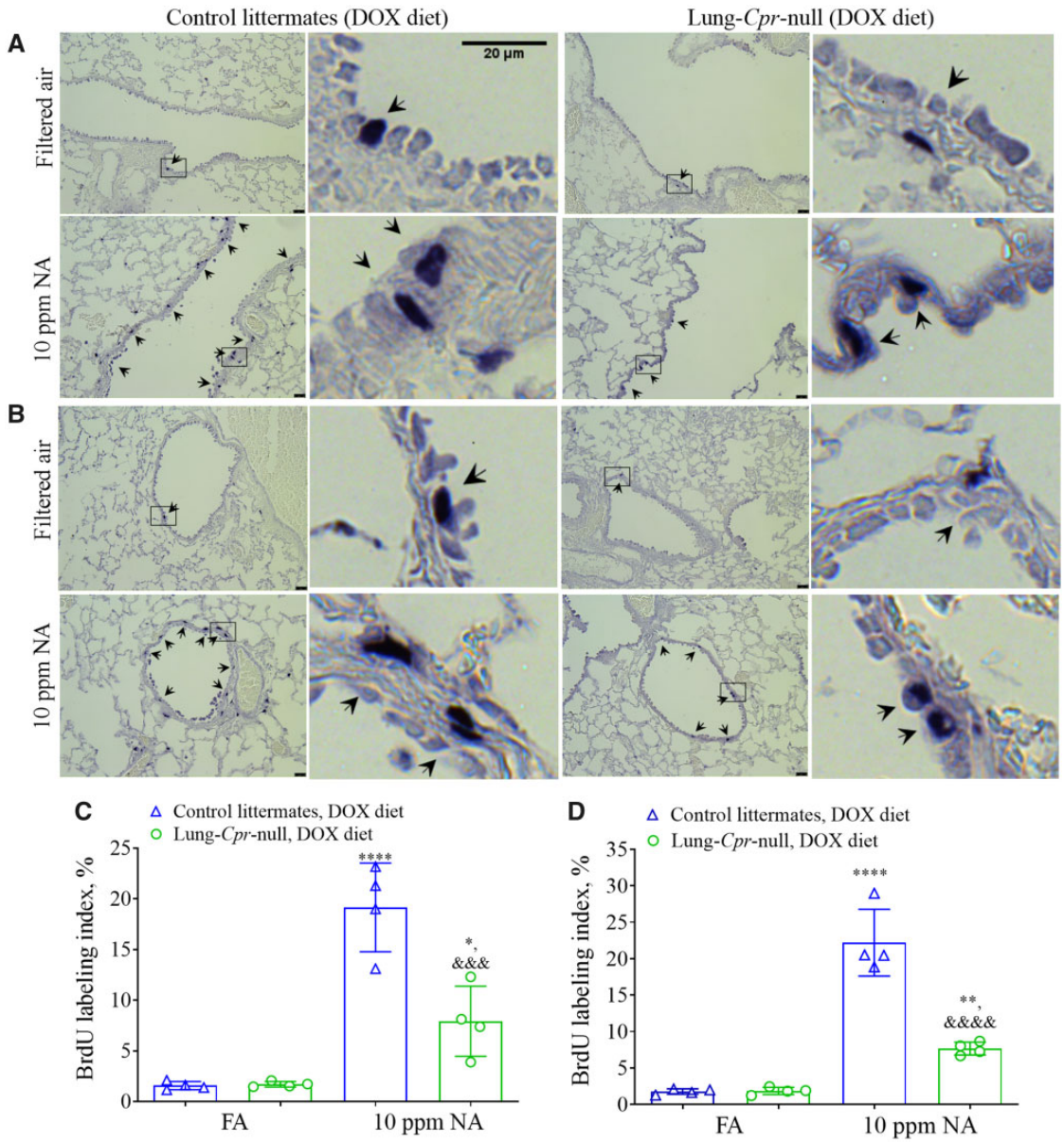

Figure 8. BrdU (5-bromo-2′-deoxyuridine) labeling index in airway epithelial cells after inhalation exposure to naphthalene (NA). Two- to 3-month-old lung-*Cpr*-null mice and their control littermates were exposed to either filtered air (FA) or 10-ppm NA for 4 h. Lungs were collected 2 days after treatment and immunohistochemically stained for nuclear incorporation of BrdU. Representative images of BrdU-positive cells (arrows) in proximal (A) and distal airways (B) are shown. Boxed areas in the left panel (Bar is 25 μm) are shown at higher magnification in the right panel (Bar is 20 μm). The proportion (%) of BrdU-positive cells (labeling index) was quantified separately for proximal (C) and distal (D) airways, as described in the Materials and Methods section. Results represent means ± SD ($n = 4$ per group). $^{\&\&\&}p < .001$, $^{\&\&\&\&}p < .0001$, by mouse genotype; $^{*}p < .05$, $^{**}p < .01$, $^{****}p < .0001$, by exposure (2-way ANOVA followed by Bonferroni's test for multiple comparisons). Abbreviation: DOX, doxycycline.

SUPPLEMENTARY DATA

Supplementary data are available at *Toxicological Sciences* online.

ACKNOWLEDGMENTS

We gratefully acknowledge the use of the services of the Histopathology Core and the Advanced Light Microscopy Core facilities of the Wadsworth Center, New York State Department of Health, Albany, New York, as well as the University of Arizona Animal Care, University of Arizona Cancer Center Tissue Acquisition & Cellular/Molecular Analysis Shared Resources, and the Imaging Core Life Sciences North.

FUNDING

National Institutes of Health (ES020867, ES023513, ES006694, CA023074).

DECLARATION OF CONFLICTING INTERESTS

The authors declared no potential conflicts of interest with respect to the research, authorship, and/or publication of this article.

REFERENCES

Abdo, K. M., Eustis, S. L., Mcdonald, M., Jokinen, M. P., Adkins, B., and Haseman, J. K. (1992). Naphthalene: A respiratory

tract toxicant and carcinogen for mice. *Inhal. Toxicol.* **4**, 393–409.

Abdo, K. M., Grumbein, S., Chou, B. J., and Herbert, R. (2001). Toxicity and carcinogenicity study in F344 rats following 2 years of whole-body exposure to naphthalene vapors. *Inhal. Toxicol.* **13**, 931–950.

Boland, B., Lin, C. Y., Morin, D., Miller, L., Plopper, C., and Buckpitt, A. (2004). Site-specific metabolism of naphthalene and 1-nitronaphthalene in dissected airways of rhesus macaques. *J. Pharmacol. Exp. Ther.* **310**, 546–554.

Buchholz, B. A., Carratt, S. A., Kuhn, E. A., Collette, N. M., Ding, X., and Van Winkle, L. S. (2019). Naphthalene DNA Adduct formation and tolerance in the lung. *Nucl. Instrum. Methods Phys. Res. B* **438**, 119–123.

Buckpitt, A., Chang, A. M., Weir, A., Van Winkle, L., Duan, X., Philpot, R., and Plopper, C. (1995). Relationship of cytochrome P450 activity to Clara cell cytotoxicity. IV. Metabolism of naphthalene and naphthalene oxide in microdissected airways from mice, rats, and hamsters. *Mol. Pharmacol.* **47**, 74–81.

Carratt, S. A., Hartog, M., Buchholz, B. A., Kuhn, E. A., Collette, N. M., Ding, X., and Van Winkle, L. S. (2019a). Naphthalene genotoxicity: DNA adducts in primate and mouse airway explants. *Toxicol. Lett.* **305**, 103–109.

Carratt, S. A., Kovalchuk, N., Ding, X., and Van Winkle, L. S. (2019b). Metabolism and lung toxicity of inhaled naphthalene: Effects of postnatal age and sex. *Toxicol. Sci.* **170**, 536–548.

Carratt, S. A., Morin, D., Buckpitt, A. R., Edwards, P. C., and Van Winkle, L. S. (2016). Naphthalene cytotoxicity in microsomal epoxide hydrolase deficient mice. *Toxicol. Lett.* **246**, 35–41.

Chichester, C. H., Buckpitt, A. R., Chang, A., and Plopper, C. G. (1994). Metabolism and cytotoxicity of naphthalene and its metabolites in isolated murine Clara cells. *Mol. Pharmacol.* **45**, 664–672.

Ding, X., Li, L., Van Winkle, L. S., and Zhang, Q.-Y. 2018. Biochemical function of the respiratory tract: Metabolism of xenobiotics. In *Comprehensive Toxicology*, 3rd ed. (C. A. McQueen, Ed.), pp. 171–193. Elsevier Ltd, Oxford.

Hokuto, I., Ikegami, M., Yoshida, M., Takeda, K., Akira, S., Perl, A. K., Hull, W. M., Wert, S. E., and Whitsett, J. A. (2004). Stat-3 is required for pulmonary homeostasis during hyperoxia. *J. Clin. Invest.* **113**, 28–37.

Hotchkiss, J. A., Harkema, J. R., and Johnson, N. F. (1997). Kinetics of nasal epithelial cell loss and proliferation in F344 rats following a single exposure to 0.5 ppm ozone. *Toxicol. Appl. Pharmacol.* **143**, 75–82.

Hu, J., Sheng, L., Li, L., Zhou, X., Xie, F., D'Agostino, J., Li, Y., and Ding, X. (2014). Essential role of the cytochrome P450 enzyme CYP2A5 in olfactory mucosal toxicity of naphthalene. *Drug Metab. Dispos.* **42**, 23–27.

IARC. Some traditional herbal medicines, some mycotoxins, naphthalene and styrene. *IARC Monogr. Eval. Carcinog. Risks Hum.* 2002; **82**, 1–556.

Kakareka, S. V., and Kukharchyk, T. I. (2003). PAH emission from the open burning of agricultural debris. *Sci. Total Environ.* **308**, 257–261.

Kovalchuk, N., Kelty, J., Li, L., Hartog, M., Zhang, Q. Y., Edwards, P., Van Winkle, L., and Ding, X. (2017). Impact of hepatic P450-mediated biotransformation on the disposition and respiratory tract toxicity of inhaled naphthalene. *Toxicol. Appl. Pharmacol.* **329**, 1–8.

Kovalchuk, N., Zhang, Q. Y., Kelty, J., Van Winkle, L., and Ding, X. (2019). Toxicokinetic interaction between hepatic disposition and pulmonary bioactivation of inhaled naphthalene studied using Cyp2abfgs-null and CYP2A13/2F1-humanized mice with deficient hepatic cytochrome P450 activity. *Drug Metab. Dispos.* **47**, 1469–1478.

Kristof, A. S., Goldberg, P., Laubach, V., and Hussain, S. N. (1998). Role of inducible nitric oxide synthase in endotoxin-induced acute lung injury. *Am. J. Respir. Crit. Care Med.* **158**, 1883–1889.

Lawson, G. W., Van Winkle, L. S., Toskala, E., Senior, R. M., Parks, W. C., and Plopper, C. G. (2002). Mouse strain modulates the role of the ciliated cell in acute tracheobronchial airway injury-distal airways. *Am. J. Pathol.* **160**, 315–327.

Li, L., Carratt, S., Hartog, M., Kovalchuk, N., Jia, K., Wang, Y., Zhang, Q.-Y., Edwards, P., Van Winkle, L., and Ding, X. (2017). Human CYP2A13 and CYP2F1 mediate naphthalene toxicity in the lung and nasal mucosa of CYP2A13/2F1-humanized mice. *Environ. Health Perspect.* **125**, 067004.

Li, L., Wei, Y., Van Winkle, L., Zhang, Q. Y., Zhou, X., Hu, J., Xie, F., Kluetzman, K., and Ding, X. (2011). Generation and characterization of a Cyp2f2-null mouse and studies on the role of CYP2F2 in naphthalene-induced toxicity in the lung and nasal olfactory mucosa. *J. Pharmacol. Exp. Ther.* **339**, 62–71.

Perl, A. K., Tichelaar, J. W., and Whitsett, J. A. (2002). Conditional gene expression in the respiratory epithelium of the mouse. *Transgenic Res.* **11**, 21–29.

Perl, A. K., Wert, S. E., Loudy, D. E., Shan, Z., Blair, P. A., and Whitsett, J. A. (2005). Conditional recombination reveals distinct subsets of epithelial cells in trachea, bronchi, and alveoli. *Am. J. Respir. Cell Mol. Biol.* **33**, 455–462.

Plopper, C. G., Macklin, J., Nishio, S. J., Hyde, D. M., and Buckpitt, A. R. (1992a). Relationship of cytochrome P-450 activity to Clara cell cytotoxicity. III. Morphometric comparison of changes in the epithelial populations of terminal bronchioles and lobar bronchi in mice, hamsters, and rats after parenteral administration of naphthalene. *Lab. Invest.* **67**, 553–565.

Plopper, C. G., Suverkropp, C., Morin, D., Nishio, S., and Buckpitt, A. (1992b). Relationship of cytochrome P-450 activity to Clara cell cytotoxicity. I. Histopathologic comparison of the respiratory tract of mice, rats and hamsters after parenteral administration of naphthalene. *J. Pharmacol. Exp. Ther.* **261**, 353–363.

Richieri, P. R., and Buckpitt, A. R. (1987). Efflux of naphthalene oxide and reactive naphthalene metabolites from isolated hepatocytes. *J. Pharmacol. Exp. Ther.* **242**, 485–492.

United States Environmental Protection Agency (USEPA). (1986). *Summary of emissions associated with sources of naphthalene*. EPA-450/3-88-003. USEPA, ResearchTriangle Park, NC.

Van Winkle, L. S., Buckpitt, A. R., Nishio, S. J., Isaac, J. M., and Plopper, C. G. (1995). Cellular response in naphthalene-induced Clara cell injury and bronchiolar epithelial repair in mice. *Am. J. Physiol.* **269**, L800–818.

Van Winkle, L. S., Buckpitt, A. R., and Plopper, C. G. (1996). Maintenance of differentiated murine Clara cells in microdissected airway cultures. *Am. J. Respir. Cell Mol. Biol.* **14**, 586–598.

Warren, D. L., Brown, D. L., and Buckpitt, A. R. (1982). Evidence for cytochrome P-450 mediated metabolism in the bronchiolar damage by naphthalene. *Chem. Biol. Interact.* **40**, 287–303.

Weng, Y., Fang, C., Turesky, R. J., Behr, M., Kaminsky, L. S., and Ding, X. (2007). Determination of the role of target tissue metabolism in lung carcinogenesis using conditional cytochrome P450 reductase-null mice. *Cancer Res.* **67**, 7825–7832.

West, J. A., Pakehham, G., Morin, D., Fleschner, C. A., Buckpitt, A. R., and Plopper, C. G. (2001). Inhaled naphthalene causes dose dependent Clara cell cytotoxicity in mice but not in rats. *Toxicol. Appl. Pharmacol.* **173**, 114–119.

Witschi, H., Espiritu, I., Maronpot, R. R., Pinkerton, K. E., and Jones, A. D. (1997). The carcinogenic potential of the gas phase of environmental tobacco smoke. *Carcinogenesis* **18**, 2035–2042.

Wu, L., Gu, J., Weng, Y., Kluetzman, K., Swiatek, P., Behr, M., Zhang, Q. Y., Zhuo, X., Xie, Q., and Ding, X. (2003). Conditional knockout of the mouse NADPH-cytochrome p450 reductase gene. *Genesis* **36**, 177–181.